

Design of a Composite Controller for a Two-Link Flexible Manipulator

Bruno Siciliano

Dipartimento di Informatica e Sistemistica, Università degli Studi di Napoli
"Federico II" Via Claudio 21, 80125 Napoli, Italy

Jonnalagadda V.R. Prasad and Anthony J. Calise

School of Aerospace Engineering, Georgia Institute of Technology, Atlanta,
Georgia 30332-0150, USA

Abstract

This paper presents the design of a composite controller for a two-time scale nonlinear model of a two-link flexible manipulator. First a slow control is designed for the slow (rigid) subsystem, then a fast stabilizing control for the fast (flexible) subsystem. In particular, the problem of lack of full state measurements concerned with the fast control design is addressed: An output feedback dynamic compensator of fixed order is designed, and its optimal gains are computed according to a loop transfer recovery technique in order to obtain a robust design. The overall control is tested by means of simulation results.

1. Introduction

Lightweight flexible arms have lately been receiving the attention of an increasing number of researchers. Potentially, they may improve on the performance of conventional massive rigid industrial manipulators. The main problem for modeling and controlling a flexible arm is induced by the structural flexibility.

Several approaches have been proposed in the literature for modeling lightweight arms. One common denominator is the adoption of the Lagrangian technique which yields closed-form expressions of all dynamic terms. As for the inherently distributed nature of the flexible system, finite-dimensional models are needed which approximate the exact infinite-dimensional models. The recursive formulation proposed by Book (1984), suitably combined with the assumed-modes method, leads to a number of generalized coordinates to handle for control purposes.

A variety of contributions aimed at designing control systems performing active feedback control of flexible vibrations have been proposed, employing linear control (Cannon and Schmitz, 1984; Hastings and Book, 1985; Oakley and Cannon, 1988), frequency domain techniques (Chait, Radcliffe, and MacCluer, 1988; Bayo et al., 1989; Yurkovich, Pacheco, and Tzes, 1989), adaptive control (Yuan, Book, and Siciliano, 1989), robust control (Korolov and Chen, 1989), transfer function approaches (Wang and Vidyasagar, 1989), inverse dynamics techniques (Asada, Ma, and Tokumaru, 1987; Bayo, Movaghar, and Medus, 1988), nonlinear decoupling controllers (Singh and Schy, 1986; De Luca and Siciliano, 1989; Pfeiffer, 1989), pseudolinearization methods (Nicosia, Tomei, and Tornambè, 1989). One limitation of most studies is that the flexible one-link case is investigated. This is much too a simple case to capture the coupling effects between rigid body and flexible body dynamics.

Here we adopt a two-time scale approach (Siciliano and Book, 1988) which allows the definition of a slow subsystem corresponding to the rigid body motion, and a fast subsystem describing the flexible motion. A composite control strategy (Kokotovic, 1984) is then applied. First a slow control is designed for the slow subsystem as it would be done for an equivalent rigid arm, then a fast control stabilizes the fast subsystem. In particular, the problem of the lack of full state availability is addressed, as the rates of the flexible variables cannot be directly measured. Preliminary work can be found in (Siciliano, Calise,

and Prasad, 1989) and in (Calise, Prasad, and Siciliano, 1990) for the simple case of a one-link flexible arm. This paper extends this approach to the case of a two-link nonlinear arm model (De Luca and Siciliano, 1990a, 1990b). A fixed order dynamic compensator for the fast subsystem is designed (Kramer and Calise, 1988) according to a loop transfer recovery formulation (Calise and Prasad, 1989) which is shown to lead to a straightforward design procedure, with excellent robustness properties. Simulation results are presented which validate the theoretical conclusions.

2. Two-Time Scale Model of a Two-Link Flexible Arm

In what follows, we consider a planar *two-link* flexible arm with rotary joints subject only to bending deformations in the plane of motion (torsional effects are neglected). A sketch of the arm with kinematic frame assignments is shown in Fig. 1. A payload is added at the tip of the outer link, while hub inertias are included at the actuated joints. Links are modeled as Euler-Bernoulli beams of uniform density with clamped-mass boundary conditions. A finite-dimensional model of link flexibility is obtained with *two* assumed modes for *each* link. The standard Lagrangian approach (Book, 1984) is followed and the resulting dynamic equations are explicated below in a form suitable to two-time scale modeling (Siciliano and Book, 1988). The reader is referred to (De Luca and Siciliano, 1990a) for the details on intermediate steps of derivation and to (De Luca and Siciliano, 1990b) for the expressions of the model coefficients.

The equations of motion can be written in the closed-form

$$\mathbf{M}(\mathbf{q}, \mathbf{d}) \begin{bmatrix} \ddot{\mathbf{q}} \\ \ddot{\mathbf{d}} \end{bmatrix} + \begin{bmatrix} \mathbf{f}_1(\mathbf{q}, \dot{\mathbf{q}}) \\ \mathbf{f}_2(\mathbf{q}, \dot{\mathbf{q}}) \end{bmatrix} + \begin{bmatrix} \mathbf{g}_1(\mathbf{q}, \dot{\mathbf{q}}, \mathbf{d}, \dot{\mathbf{d}}) \\ \mathbf{g}_2(\mathbf{q}, \dot{\mathbf{q}}, \mathbf{d}, \dot{\mathbf{d}}) \end{bmatrix} + \begin{bmatrix} \mathbf{0} \\ \mathbf{Kd} \end{bmatrix} = \begin{bmatrix} \mathbf{u} \\ \mathbf{0} \end{bmatrix} \quad (1)$$

where $\mathbf{q} = (q_1 \ q_2)^T$ is the vector of joint variables, \mathbf{M} is the inertia matrix, \mathbf{f}_1 and \mathbf{f}_2 are the vectors containing gravitational, Coriolis, and centrifugal terms, \mathbf{g}_1 and \mathbf{g}_2 are the vectors accounting for the interaction of joint variables and their rates with deflection variables and their rates, $\mathbf{K} = \text{diag}(k_{11}, k_{12}, k_{21}, k_{22})$ is the positive diagonal matrix of the constant flexural stiffness coefficients, $\mathbf{u} = (u_1 \ u_2)^T$ is the vector of input torques applied at the joints. Two null vectors of appropriate dimensions appear in (1). As for the vector of deflection variables $\mathbf{d} = (d_{11} \ d_{12} \ d_{21} \ d_{22})^T$, this is obtained as the result of an assumed modes expansion for each link — under the assumption of small deflections — truncated at two modes for each link (Meirovitch, 1967). Also, note that, in force of the clamped boundary condition, there is no modal displacements at joint locations and then zero input torques; this is even enforced under joint feedback control (Cetinkunt and Book, 1990).

Since the inertia matrix \mathbf{M} is symmetric and positive-definite, it can be inverted and denoted by \mathbf{H} , which can be partitioned as follows:

$$\mathbf{H} = \begin{bmatrix} \mathbf{H}_{11} [2 \times 2] & \mathbf{H}_{12} [2 \times 4] \\ \mathbf{H}_{21} [4 \times 2] & \mathbf{H}_{22} [4 \times 4] \end{bmatrix}. \quad (2)$$

Equations (1) then become — dropping the dependences for notation compactness —

$$\ddot{\mathbf{q}} = -\mathbf{H}_{11}\mathbf{f}_1 - \mathbf{H}_{12}\mathbf{f}_2 - \mathbf{H}_{11}\mathbf{g}_1 - \mathbf{H}_{12}\mathbf{g}_2 - \mathbf{H}_{12}\mathbf{Kd} + \mathbf{H}_{11}\mathbf{u}, \quad (3a)$$

$$\ddot{\mathbf{d}} = -\mathbf{H}_{21}\mathbf{f}_1 - \mathbf{H}_{22}\mathbf{f}_2 - \mathbf{H}_{21}\mathbf{g}_1 - \mathbf{H}_{22}\mathbf{g}_2 - \mathbf{H}_{22}\mathbf{Kd} + \mathbf{H}_{21}\mathbf{u}. \quad (3b)$$

The system (3) is characterized by having *six* generalized coordinates but only *two* control inputs. This poses serious drawbacks for control design purposes, compared to the case of rigid arms.

A viable strategy is represented by a singular perturbation approach (Siciliano and Book, 1988), according to which a two-time scale description of the system is obtained. Specifically, the smallest stiffness constant of \mathbf{K} in (1), say k_{11} , can be regarded as the inverse of a perturbation parameter, i.e.

$\mu = 1/k_{11}$. For a given manipulator geometry, the limit $\mu \rightarrow 0$ corresponds to the case of an equivalent rigid manipulator. Therefore, factoring K as $K = \tilde{K}/\mu$ and defining the new variables (elastic forces)

$$\mathbf{z} := \frac{1}{\mu} \tilde{K} \mathbf{d} \quad (4)$$

yields the equations of the system in two-time-scale form

$$\ddot{\mathbf{q}} = -\mathbf{H}_{11} \mathbf{f}_1 - \mathbf{H}_{12} \mathbf{f}_2 - \mathbf{H}_{11} \mathbf{g}_1 - \mathbf{H}_{12} \mathbf{g}_2 - \mathbf{H}_{12} \mathbf{z} + \mathbf{H}_{11} \mathbf{u}, \quad (5a)$$

$$\mu \ddot{\mathbf{z}} = -\mathbf{H}'_{21} \mathbf{f}_1 - \mathbf{H}'_{22} \mathbf{f}_2 - \mathbf{H}'_{21} \mathbf{g}_1 - \mathbf{H}'_{22} \mathbf{g}_2 - \mathbf{H}'_{22} \mathbf{z} + \mathbf{H}'_{21} \mathbf{u}. \quad (5b)$$

where the superscript "prime" in (5b) indicates that the corresponding quantities have been premultiplied by \tilde{K} .

At this point, the typical steps of a singular perturbation formulation can be taken (Kokotovic, 1984). Because of the presence of μ , the system described by equations (5) exhibits a boundary layer phenomenon in the fast variables \mathbf{z} . Formally setting $\mu = 0$ accomplishes a model order reduction from $n + m'$ to n . It can be shown (Siciliano and Book, 1988) that $\mathbf{g}_1(\mu = 0) = \mathbf{0}$ and $\mathbf{g}_2(\mu = 0) = \mathbf{0}$. The differential equations (5b) degenerate into the algebraic transcendental equations

$$\mathbf{0} = -\mathbf{H}'_{21,s} \mathbf{f}_{1,s} - \mathbf{H}'_{22,s} \mathbf{f}_{2,s} - \mathbf{H}'_{22,s} \mathbf{z}_s + \mathbf{H}'_{21,s} \mathbf{u}_s \quad (6)$$

where the subscript "s" indicates that the corresponding quantities are computed in the slow time scale, i.e. for $\mu = 0$. Since $\mathbf{H}'_{22,s}$ is positive definite, it is possible to solve equations (6) for \mathbf{z}_s as

$$\mathbf{z}_s = \mathbf{H}'_{22,s} (-\mathbf{H}'_{21,s} \mathbf{f}_{1,s} + \mathbf{H}'_{21,s} \mathbf{u}_s) - \mathbf{f}_{2,s}. \quad (7)$$

Using this solution in (5a) formally yields the slow subsystem

$$\ddot{\mathbf{q}}_s = (\mathbf{H}_{11,s} - \mathbf{H}_{12,s} \mathbf{H}'_{22,s}^{-1} \mathbf{H}'_{21,s}) (-\mathbf{f}_{1,s} + \mathbf{u}_s). \quad (8)$$

It can easily be checked that

$$\mathbf{H}_{11,s} - \mathbf{H}_{12,s} \mathbf{H}'_{22,s}^{-1} \mathbf{H}'_{21,s} = \mathbf{M}_{11,s}^{-1} \quad (9)$$

where $\mathbf{M}_{11,s}$ is the (2×2) positive definite matrix appearing in the model of the equivalent rigid arm.

To derive the fast (boundary-layer) subsystem, the slow variables are treated as constants. Defining the fast variables $\mathbf{z}_f = \mathbf{z} - \mathbf{z}_s$, and the fast control $\mathbf{u}_f = \mathbf{u} - \mathbf{u}_s$, the fast subsystem of (5b) becomes

$$\frac{d^2 \mathbf{z}_f}{d\tau^2} = -\mathbf{H}'_{22,s} \mathbf{z}_f + \mathbf{H}'_{21,s} \mathbf{u}_f \quad (10)$$

where $\tau = t/\sqrt{\mu}$ is the fast time scale.

3. Design of a Composite Controller with Fast Output Feedback

On the basis of the above two-time scale model, the design of a feedback controller for the system (5) can be performed according to a composite strategy (Kokotovic 1984); namely

$$\mathbf{u} = \mathbf{u}_s(\mathbf{q}, \dot{\mathbf{q}}) + \mathbf{u}_f(\mathbf{z}_f, \frac{d\mathbf{z}_f}{d\tau}) \quad (11)$$

with the constraint that $\mathbf{u}_f(0, 0) = \mathbf{0}$, so that \mathbf{u}_f is inactive along the trajectories specified by (7).

The slow control for the slow subsystem (8) can be designed according to the well-known computed-torque concept used for rigid manipulators,

$$\mathbf{u}_s = \hat{\mathbf{M}}_{11,s} \mathbf{v} + \hat{\mathbf{f}}_{1,s} \quad (12)$$

where $\hat{\mathbf{M}}_{11,s}$ and $\hat{\mathbf{f}}_{1,s}$ denote the available estimates of $\mathbf{M}_{11,s}$ and $\mathbf{f}_{1,s}$, respectively, and \mathbf{v} is a new control input. This can be chosen as

$$\mathbf{v} = \ddot{\mathbf{q}}_d + \mathbf{K}_D \dot{\mathbf{e}} + \mathbf{K}_P \mathbf{e} \quad (13a)$$

where \mathbf{q}_d is the desired joint trajectory, $\mathbf{e} = \mathbf{q}_d - \mathbf{q}$, and \mathbf{K}_P , \mathbf{K}_D are suitable positive diagonal matrices which, under the assumption of perfect compensation ($\hat{\mathbf{M}}_{11,s} = \mathbf{M}_{11,s}$, $\hat{\mathbf{f}}_{1,s} = \mathbf{f}_{1,s}$) shape the response of the linear stable system

$$\ddot{\mathbf{e}} + \mathbf{K}_D \dot{\mathbf{e}} + \mathbf{K}_P \mathbf{e} = \mathbf{0}. \quad (13b)$$

At this point, it is required that the fast subsystem (10) be uniformly stable along the trajectories \mathbf{z}_s given by (7). To this purpose, let a state space representation of (10) be

$$\dot{\mathbf{x}} = \mathbf{A}\mathbf{x} + \mathbf{B}\mathbf{u}_f \quad (14a)$$

$$\mathbf{A}_{[s \times s]} = \begin{bmatrix} \mathbf{O} & \mathbf{I} \\ -\mathbf{H}'_{22,s} & \mathbf{O} \end{bmatrix} \quad \mathbf{B}_{[s \times 2]} = \begin{bmatrix} \mathbf{O} \\ \mathbf{H}'_{21,s} \end{bmatrix} \quad (14b)$$

where $\mathbf{x}^T = [\mathbf{z}_f^T (dz_f/dr)^T]$, and zero block matrices of appropriate dimensions appear. The system described by equations (14) is a linear system with m' couples of poles on the imaginary axis in the s -plane. Since the pair (\mathbf{A}, \mathbf{B}) can be shown to be completely controllable, a fast state feedback control of the type

$$\mathbf{u}_f = \mathbf{K}_P \mathbf{z}_f + \mathbf{K}_D \frac{d\mathbf{z}_f}{dr} \quad (15)$$

can be devised to arbitrarily place the poles of the system (14). This would require, however, full state availability. In practice, Hastings and Book (1985) showed that the deflection variables \mathbf{d} can be accurately reconstructed from strain gage measurements, whereas their rates $\dot{\mathbf{d}}$ cannot. In order to overcome this drawback, in the following an output feedback controller for the fast subsystem (14) is developed which is based on the design of an optimal fixed-order compensator

Kramer and Calise (1988) showed two canonical forms for the compensator representation which provide a minimal parameterization. These representations exclude the use of direct feedthrough of the output, since direct feedback is undesirable both from the point of view of sensor noise reduction and robustness. Also, a loop transfer recovery procedure for fixed-order compensators was proposed by Calise and Prasad (1989) which uniquely defines the state and compensator weighting matrix, and the initial state distribution matrix. Below we adopt this formulation for the design of the output fast feedback controller.

The output equation for the fast subsystem (14) can be simply expressed as

$$\mathbf{y} = \mathbf{C}\mathbf{x} \quad (16a)$$

$$\mathbf{C}_{[4 \times s]} = [\mathbf{I} \quad \mathbf{O}] \quad (16b)$$

where the identity matrix \mathbf{I} and the null matrix \mathbf{O} account for the fact the variables \mathbf{z}_f are available while their rates $d\mathbf{z}_f/dr$ are not.

A compensator of fixed order p , without direct feedthrough of the output, can be formulated in observer canonical form as

$$\mathbf{u}_t = -\mathbf{H}^0 \mathbf{w} \quad (17a)$$

$$\dot{\mathbf{w}} = \mathbf{P}^0 \mathbf{w} + \mathbf{u}_p \quad (17b)$$

$$\mathbf{u}_p = \mathbf{P}_w \mathbf{u}_t - \mathbf{N} \mathbf{y} \quad (17c)$$

where

$$\mathbf{H}_{[2 \times p]}^0 = \text{block diag}[(0, \dots, 0, 1)_{(\ell_i \times 1)}, i = 1, 2] \quad (18)$$

and

$$\mathbf{P}_{[p \times p]}^0 = \text{block diag}[\mathbf{P}_1^0, \mathbf{P}_2^0] \quad (19a)$$

$$\mathbf{P}_{i, [\ell_i \times \ell_i]}^0 = \begin{bmatrix} 0 & 0 & \dots & 0 & 0 \\ 1 & 0 & \dots & 0 & 0 \\ 0 & 1 & \dots & 0 & 0 \\ \vdots & \vdots & \ddots & \vdots & \vdots \\ 0 & 0 & \dots & 1 & 0 \end{bmatrix} \quad (19b)$$

with the observability indices ℓ_i satisfying the following conditions: $\ell_1 + \ell_2 = p$, and $\ell_1 < \ell_2$. In (17c), \mathbf{N} and \mathbf{P}_w are respectively a $(p \times 4)$ matrix and a $(p \times 2)$ matrix of free parameters.

Defining $\tilde{\mathbf{x}}^T = (\mathbf{x}^T \mathbf{w}^T)$, $\tilde{\mathbf{y}}^T = (\mathbf{y}^T - \mathbf{u}_t^T)$, and $\tilde{\mathbf{u}} = \mathbf{u}_p$, the dynamic compensator design can be expressed in terms of a standard output feedback problem for the augmented system

$$\dot{\tilde{\mathbf{x}}} = \tilde{\mathbf{A}} \tilde{\mathbf{x}} + \tilde{\mathbf{B}} \tilde{\mathbf{u}} \quad (20a)$$

$$\tilde{\mathbf{y}} = \tilde{\mathbf{C}} \tilde{\mathbf{x}} \quad (20b)$$

$$\tilde{\mathbf{u}} = -\mathbf{G} \tilde{\mathbf{y}} \quad (20c)$$

$$\tilde{\mathbf{A}}_{[(s+p) \times (s+p)]} = \begin{bmatrix} \mathbf{A} & -\mathbf{B}\mathbf{H}^0 \\ \mathbf{O} & \mathbf{P}^0 \end{bmatrix} \quad \tilde{\mathbf{B}}_{[(s+p) \times p]} = \begin{bmatrix} \mathbf{O} \\ \mathbf{I} \end{bmatrix} \quad (20d)$$

$$\tilde{\mathbf{C}}_{[p \times (s+p)]} = \begin{bmatrix} \mathbf{C} & \mathbf{O} \\ \mathbf{O} & \mathbf{H}^0 \end{bmatrix} \quad \mathbf{G}_{[p \times p]} = [\mathbf{N} \quad \mathbf{P}_w] \quad (20e)$$

where the number of free parameters is minimized and no zero elements in \mathbf{G} appear.

The output feedback problem is then optimized according to the following augmented quadratic performance index

$$J = E_{\tilde{\mathbf{x}}_0} \left[\int_0^\infty (\tilde{\mathbf{x}}^T \mathbf{Q} \tilde{\mathbf{x}} + \tilde{\mathbf{u}}^T \mathbf{R} \tilde{\mathbf{u}}) dt \right] \quad (21)$$

where $\mathbf{Q} \geq \mathbf{O}$ and $\mathbf{R} > \mathbf{O}$, and the expectation is taken over some initial distribution on $\tilde{\mathbf{x}}_0$.

The necessary conditions for optimality require the solution of the triple $(\mathbf{G}, \mathbf{S}, \mathbf{L})$ satisfying:

$$\mathbf{A}_c^T \mathbf{S} + \mathbf{S} \mathbf{A}_c + \mathbf{Q} + \tilde{\mathbf{C}}^T \mathbf{G}^T \mathbf{R} \mathbf{G} \tilde{\mathbf{C}} = \mathbf{O} \quad (22a)$$

$$\mathbf{A}_c \mathbf{L} + \mathbf{L} \mathbf{A}_c^T + \tilde{\mathbf{X}}_0 = \mathbf{O} \quad (22b)$$

$$\mathbf{R} \mathbf{G} \tilde{\mathbf{C}} \mathbf{L} \tilde{\mathbf{C}}^T - \tilde{\mathbf{B}}^T \mathbf{S} \mathbf{L} \tilde{\mathbf{C}}^T = \mathbf{O} \quad (22c)$$

for a stable closed-loop system matrix

$$\mathbf{A}_c = \tilde{\mathbf{A}} - \tilde{\mathbf{B}} \mathbf{G} \tilde{\mathbf{C}} \quad (23)$$

In (22b), $\tilde{\mathbf{X}}_0 = E[\tilde{\mathbf{x}}_0 \tilde{\mathbf{x}}_0^T]$ is the variance matrix associated with the distribution assumed for the initial conditions. The convergent algorithm proposed by Moerder and Calise (1985) can be employed for solving (22a-22c).

Full state feedback design is often used as a first step in designing an output feedback controller. If the fixed order compensator is designed to approximate the loop transfer properties of the full state design, then the closed-loop system should contain a set of eigenvalues and eigenvectors that approximate those of the full state design. The return vector in the case of full state design is $-\mathbf{K}^* \mathbf{x}$, where \mathbf{K}^* is the optimal gain matrix specified as in (15), i.e. $\mathbf{K}^* = [\mathbf{K}_{F1} \ \mathbf{K}_{D1}]$. Referring to (17a), the return vector in the case of fixed-order compensator design is $-\mathbf{H}^0 \mathbf{w}$. Thus, as in (Calise and Prasad, 1989), the objective in designing the compensator should be to minimize

$$\mathbf{y}_1 = \mathbf{K}^* \mathbf{x} - \mathbf{H}^0 \mathbf{w} \quad (24)$$

for a suitably chosen input and for zero initial conditions. This naturally leads to selecting the following index of performance:

$$J = E_{\tilde{\mathbf{x}}_0} \left[\int_0^{\infty} (\mathbf{y}_1^T \mathbf{y}_1 + \tilde{\mathbf{u}}^T \tilde{\mathbf{u}}) dt \right]. \quad (25)$$

Substituting for \mathbf{y}_1 from (24), and rewriting (25) in the form of (21) leads to the following expressions for the weighting matrices:

$$\mathbf{Q} = \begin{bmatrix} \mathbf{K}^* \mathbf{K}^{*T} & -\mathbf{K}^* \mathbf{H}^0 \\ -\mathbf{H}^0 \mathbf{K}^{*T} & \mathbf{H}^0{}^T \mathbf{H}^0 \end{bmatrix} \quad \mathbf{R} = \rho \mathbf{I}. \quad (26)$$

Selecting the input waveforms as impulses with magnitudes uniformly distributed on the unit sphere results in the following expression for $\tilde{\mathbf{X}}_0$:

$$\tilde{\mathbf{X}}_0 = \begin{bmatrix} \mathbf{B}\mathbf{B}^T & \mathbf{O} \\ \mathbf{O} & \mathbf{O} \end{bmatrix}. \quad (27)$$

Equations (26) and (27) uniquely define the structure of the weighting matrices needed for the fixed-order compensator design. Notice that, unlike the design of a full-order observer, the design of a fixed-order compensator depends on the gain matrix from the full state design. Moreover, this gain matrix is not implemented as a part of the final controller.

4. A Case Study

A numerical case study is developed to illustrate the effectiveness of the design procedure outlined in the previous section. The physical parameters of the arm with uniform mass link density are:

- link lengths: 1 m
- link masses: 1 m
- 2nd-link center of mass: 0.5 m
- 2nd-joint hub mass: 0.2 kg
- payload mass: 0.1 kg
- link inertias: 0.066 kg m²
- hub inertias: 0.1 kg m²
- payload inertia: 0.0005 kg m²
- link flexural rigidities: 1 N m²

With these data, the perturbation parameter in (4) turns out $\mu = 0.0503$ justifying the two-time scale separation.

A composite control is designed first, which is composed of a slow control as in (12,13) and a fast full state feedback control as in (15). Perfect compensation is assumed in (12), and the feedback matrices in (13) are chosen as $K_P = 2.25I$ and $K_D = 3I$, corresponding to a double pole at -1.5 for the error dynamics at both joints. Then, a full state feedback design is carried out to stabilize the two fast modes at each link. In the open-loop, the modes have zero damping with natural frequencies at 10.3, 13.6, 67.4, 85.3 rad/s. Thus, the above choice for the slow control poles preserves the time-scale separation between the slow and the fast subsystem which is crucial for the applicability of the singular perturbation approach. A standard LQR design is undertaken for the nominal configuration of the arm with $q_2 = 0$;* the matrices $H'_{22,s}$ and $H'_{21,s}$ in (14b) take on the following values:

$$H'_{22,s} = \begin{bmatrix} 3.17 \times 10^2 & -3.15 \times 10^2 & -5.30 & -2.55 \\ -4.60 \times 10^3 & 7.06 \times 10^3 & 4.83 \times 10^1 & 2.33 \times 10^1 \\ -7.17 \times 10^1 & 4.47 \times 10^1 & 1.91 \times 10^2 & 2.04 \times 10^1 \\ -2.17 \times 10^3 & 1.35 \times 10^3 & 1.28 \times 10^3 & 4.54 \times 10^3 \end{bmatrix}$$

$$H'_{21,s} = \begin{bmatrix} -2.27 \times 10^1 & -3.59 \times 10^2 \\ -1.93 \times 10^2 & 7.46 \times 10^3 \\ -2.06 \times 10^{-1} & -5.40 \times 10^1 \\ -6.26 & 1.07 \times 10^3 \end{bmatrix}$$

The weighting matrices are set to $\text{diag}(0,0,0,0,0.015,0,0.005,0.0005)$ and $\text{diag}(1,1)$. The resulting feedback gain matrices as in (15) are:

$$K_{Pf} = \begin{bmatrix} 4.13 \times 10^{-2} & -1.99 \times 10^{-2} & -9.06 \times 10^{-2} & -4.25 \times 10^{-2} \\ -4.38 \times 10^{-1} & -2.02 \times 10^{-1} & 5.29 \times 10^{-1} & 1.33 \end{bmatrix}$$

$$K_{Df} = \begin{bmatrix} -1.10 \times 10^{-1} & -5.42 \times 10^{-3} & 1.31 \times 10^{-2} & 4.05 \times 10^{-4} \\ -3.85 \times 10^{-2} & 1.15 \times 10^{-2} & -7.21 \times 10^{-2} & -1.01 \times 10^{-1} \end{bmatrix}$$

which achieve damping ratios of 0.23, 0.25, 0.22, 0.31 for the four modes.

Next, an output fast feedback design with fourth-order compensation — $p = 4$ in (17) — is carried out. The above full state feedback gain matrices are used to compute Q in (26), while $\rho = 1.0 \times 10^{-6}$. The design results in damping ratios of 0.17, 0.25, 0.25, 0.26 for the four modes, with the gain matrix in (20e) being formed by:

$$N = \begin{bmatrix} 3.07 \times 10^4 & -1.19 \times 10^3 & 1.08 \times 10^3 & -1.95 \times 10^3 \\ -2.95 \times 10^3 & 1.07 \times 10^3 & -1.67 \times 10^3 & 5.89 \times 10^2 \\ 1.05 \times 10^3 & -3.87 \times 10^2 & 4.50 \times 10^2 & -4.74 \times 10^2 \\ 1.88 \times 10^4 & -6.83 \times 10^3 & 1.07 \times 10^4 & -3.84 \times 10^3 \end{bmatrix}$$

$$P_w = \begin{bmatrix} -9.28 \times 10^3 & -1.04 \times 10^3 \\ 9.88 \times 10^3 & 1.42 \times 10^3 \\ -3.28 \times 10^3 & -3.97 \times 10^3 \\ -6.26 \times 10^4 & -8.94 \times 10^3 \end{bmatrix}$$

Fig. 2a illustrates the extent of recovery achieved by the output feedback design. Shown is a comparison of the singular value plots for the return difference matrix with the loop broken at the input to the plant dynamics of the fast subsystem. An expanded view of the minimum singular value plots of Fig. 2a is shown in Fig. 2b. For the full state feedback design, the minimum singular value over all frequencies is

* The arm dynamics does not depend on the first joint variable (De Luca and Siciliano, 1990b).

greater than or equal to 1.0. This ensures multivariable gain and phase margins of $-6 \text{ dB} < GM < \infty$ and $-60^\circ < PM < 60^\circ$. The minimum singular value for the fourth order compensator reaches a lower bound of 0.65 — 0.6 is generally regarded as a good design value for practical applications — at a frequency of 7.2 rad/s. This corresponds to multivariable gain and phase margins of $-4.4 \text{ dB} < GM < 9.2 \text{ dB}$ and $-38^\circ < PM < 38^\circ$.

In the following, a set of simulation is presented. A joint motion is commanded from $q_d(0) = (0 - \pi/2)^T \text{ rad}$ to $q_d(T) = (0 \ 0)^T \text{ rad}$ with the velocity profile $\dot{q}_{d2}(t) = (\pi/2)[1 + \sin(2\pi t/T - \pi/2)] \text{ rad/s}$, $0 \leq t \leq T$, with $T = 4 \text{ s}$. A fifth order Runge-Kutta-Merson method has been implemented to integrate the nonlinear differential equations (1) with a sampling rate for the controller of $1.0 \times 10^{-3} \text{ s}$.

Three controllers have been applied; the slow control, the composite control with full state fast feedback, and the composite control with output fast feedback.

The results in Fig. 3 and 4 indicate that with the slow control, the performance of the arm joints is acceptable while that of the tip is not; the y -component of the tip keeps vibrating about the final target position while the x -component is quite unaffected by the imposed motion. Notice, also, the typical non-minimum phase response of the tip.

With the introduction of the fast control with full state feedback, the vibratory motion of the arm tip tends to die out (Fig. 6), without appreciably modifying the joint arm motion (Fig. 5).

Finally, the results in Fig. 7 and 8 demonstrate that the performance obtained by replacing the full state design with the output feedback design is still satisfactory.

5. Conclusions

A two-time scale approach has been developed for the control of a two-link flexible arms. The design of a composite control has been presented: This consists of a slow control design that can be performed as for the equivalent rigid arm, and of a fast control design for a simple linear system describing the flexible dynamics. The problem of lack of full state measurements has successfully been solved by adopting a fixed-order dynamic compensator design combined with the loop transfer recovery technique. The simulated case study has illustrated the effectiveness of the formulation and overall design methodology.

Acknowledgements

This work is based on research supported by *Ministero dell'Università e della Ricerca Scientifica e Tecnologica* under 40% funds, and by *US Army Research Office* under contract no. DAAL3-88-C-0003.

References

- Asada, H., Ma, Z.-D., and Tokumaru, H., 1987, "Inverse dynamics of flexible robot arms for trajectory control," *Proc. ASME Winter Annual Meet.*, Boston, MA, Vol. 6, pp. 329-336.
- Bayo, E., Movaghar, R., and Medus, M., 1988, "Inverse dynamics of a single-link flexible robot. Analytical and experimental results," *Int. J. of Robotics and Automation*, Vol. 4, pp. 63-75.
- Bayo, E., Papadopoulos, P., Stubbe, J., and Serna, M., 1989, "Inverse dynamics and kinematics of multi-link elastic robots. An iterative frequency domain approach," *Int. J. of Robotics Research*, Vol. 8, No. 6, pp. 49-62.
- Book, W.J., 1984, "Recursive Lagrangian dynamics of flexible manipulator arms," *Int. J. of Robotics Research*, Vol. 3, No. 3, pp. 87-101.
- Calise, A.J. and Prasad, J.V.R., 1990, "An approximate loop transfer recovery method for designing fixed-order compensators," *AIAA J. of Guidance, Control, and Dynamics*, Vol. 13, pp. 297-302.
- Calise, A.J., Prasad, J.V.R., and Siciliano, B., 1990, "Design of optimal output feedback compensators in two-time scale systems," *IEEE Trans. on Automatic Control*, Vol. AC-35, pp. 488-492.

Cannon, R.H. and Schmitz, E., 1984, "Initial experiments on the end-point control of a flexible one-link robot," *Int. J. of Robotics Research*, Vol. 3, No. 3, pp. 62-75.

Cetinkunt, S. and Book, W.J., 1990, "Performance limitations of joint variable-feedback controllers due to manipulator structural flexibility," *IEEE Trans. on Robotics and Automation*, Vol. RA-6, pp. 219-231.

Chait, Y., Radcliffe, C.J., and MacCluer, C.R., 1988, "Frequency domain stability criterion for vibration control of the Bernoulli-Euler beam," *ASME J. of Dynamic Systems, Measurement, and Control*, Vol. 110, pp. 303-307.

De Luca, A. and Siciliano, B., 1989, "Trajectory control of a non-linear one-link flexible arm," *Int. J. of Control*, Vol. 50, pp. 1699-1715.

De Luca, A. and Siciliano, B., 1990a, "Dynamic modelling of multi-link flexible robot arms," *Prep. IFIP Int. Conf. on Modelling the Innovation*, Roma, I, pp. 157-164.

De Luca, A. and Siciliano, B., 1990b, "Explicit dynamic modeling of a planar two-link flexible manipulator," *Proc. 29th IEEE Conf. on Decision and Control*, Honolulu, HI.

Hastings, G.G. and Book, W.J., 1985, "Experiments in optimal control of a flexible arm," *Proc. 1985 Amer. Control Conf.*, Boston, MA, pp. 728-729.

Kokotovic, P.V., 1984, "Applications of singular perturbation techniques to control problems," *SIAM Review*, Vol. 26, pp. 501-550.

Korolov, V.V., and Chen, Y.H., 1989, "Controller design robust to frequency variations in a one-link flexible robot," *ASME J. of Dynamic Systems, Measurement, and Control*, Vol. 111, pp. 1-14.

Kramer, F.S. and Calise, A.J., 1988, "Fixed order dynamic compensation for multivariable linear systems," *AIAA J. of Guidance, Control, and Dynamics*, Vol. 11, pp. 80-85.

Meirovitch, L., 1967, *Analytical Methods in Vibrations*, New York: Macmillan.

Moerder, D.D. and Calise, A.J., 1985, "Convergence of a numerical algorithm for calculating optimal output feedback gains," *IEEE Trans. on Automatic Control*, Vol. AC-30, pp. 900-903.

Nicosia, S., Tomei, P., and Tornambè, A., 1989, "Hamiltonian description and dynamic control of flexible robots," *J. of Robotic Systems*, Vol. 6, pp. 345-3616.

Oakley, C.M. and Cannon, R.H., 1988, "Initial experiments on the control of a two-link manipulator with a very flexible forearm," *Proc. 1988 Amer. Control Conf.*, Atlanta, GA, pp. 996-1002.

Pfeiffer, F., 1989, "A feedforward decoupling concept for the control of elastic robots," *J. of Robotic Systems*, Vol. 6, pp. 407-416.

Siciliano, B. and Book, W.J., 1988, "A singular perturbation approach to control of lightweight flexible manipulators," *Int. J. of Robotics Research*, Vol. 7, No. 4, pp. 79-90.

Siciliano, B., Calise, A.J., and Prasad, J.V.R., 1989, "Two-time scale stabilization of a flexible arm with output feedback," *Proc. 1989 Amer. Control Conf.*, Pittsburgh, PA, pp. 2377-2382.

Singh, S.N. and Schy, A.A., 1986, "Elastic robot control: Nonlinear inversion and linear stabilization," *IEEE Trans. on Aerospace and Electronic Systems*, Vol. AES-22, pp. 340-348.

Wang, D. and Vidyasagar, M., 1989, "Transfer function for a single flexible link," *Proc. 1989 IEEE Int. Conf. on Robotics and Automation*, Scottsdale, AZ, pp. 1042-1047.

Yuan, B.-S., Book, W.J., and Siciliano, B., 1989, "Direct adaptive control of a one-link flexible arm with tracking," *J. of Robotic Systems*, Vol. 6, pp. 663-680.

Yurkovich, S., Pacheco, F.E., and Tzes, A.P., 1989, "On-line frequency domain information for control of a flexible-link robot with varying payload," *IEEE Trans. on Automatic Control*, Vol. AC-34, pp. 1300-1304.

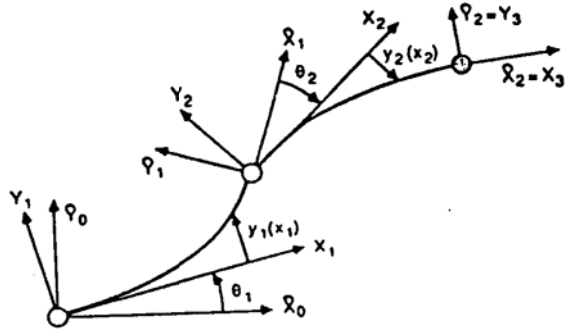


Fig. 1 — The planar two-link flexible arm

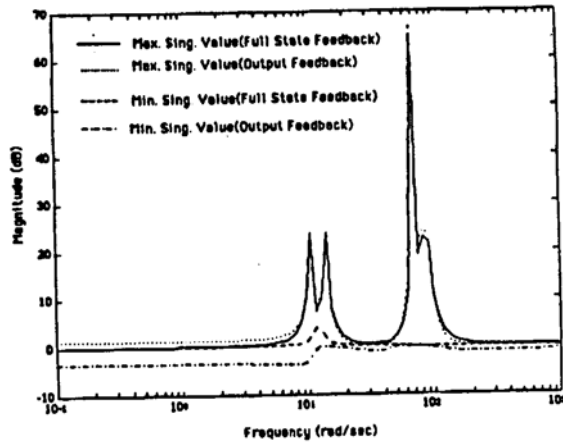


Fig. 2a — Singular value plot of the return difference matrix

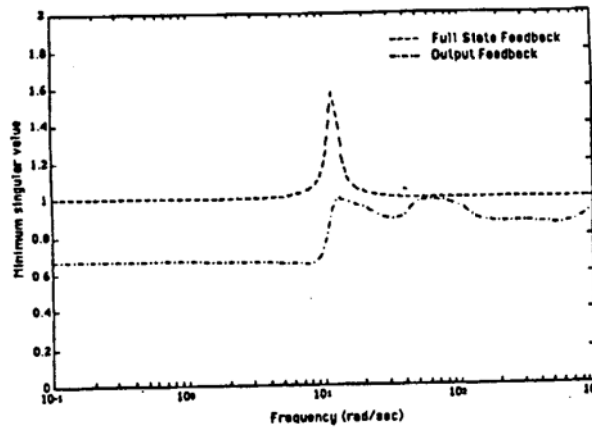


Fig. 2b — Minimum singular value plot of the return difference matrix

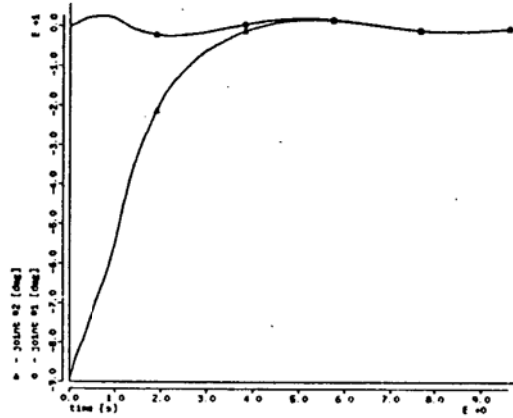


Fig. 3 — Time history of joints with slow control

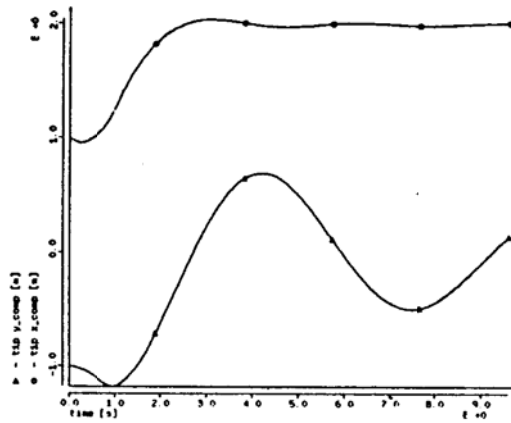


Fig. 4 — Time history of tip with slow control

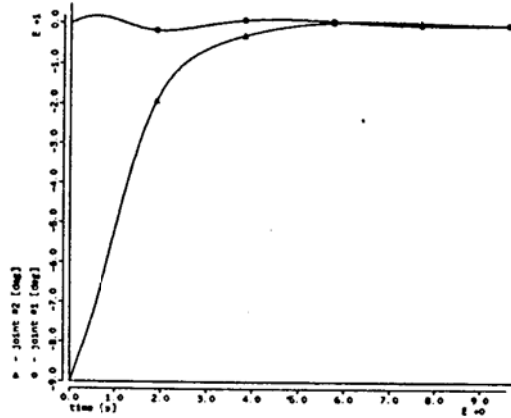


Fig. 5 — Time history of joints with composite full state feedback control

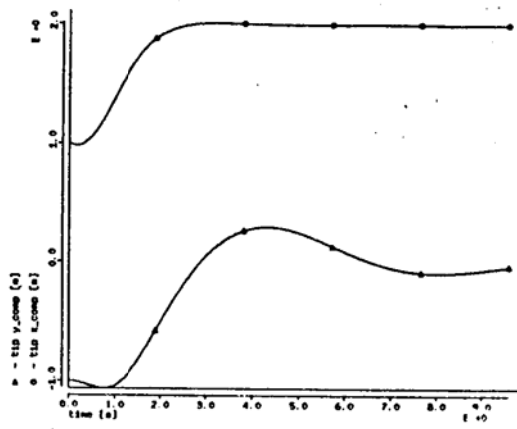


Fig. 6 — Time history of tip with composite full state feedback control

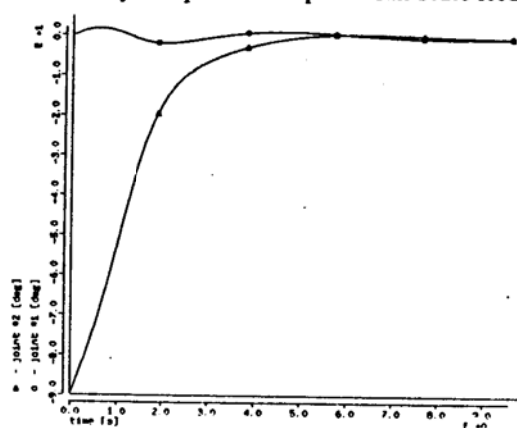


Fig. 7 — Time history of joints with composite output feedback control

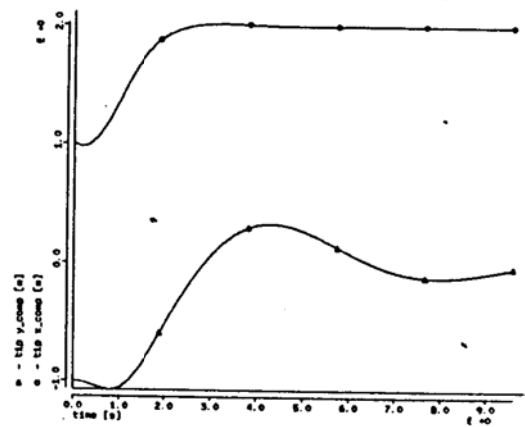


Fig. 8 — Time history of tip with composite output feedback control